5-2021

Optimality of Delaunay Triangulations

Estefania A. Sierra
The University of Texas Rio Grande Valley

OPTIMALITY OF DELAUNAY TRIANGULATIONS

A Thesis

by

ESTEFANIA A. SIERRA

Submitted to the Graduate College of
The University of Texas Rio Grande Valley
In partial fulfillment of the requirements for the degree of

MASTER OF SCIENCE

May 2021

Major Subject: Applied Mathematics

OPTIMALITY OF DELAUNAY TRIANGULATIONS

A Thesis
by
ESTEFANIA A. SIERRA

COMMITTEE MEMBERS

Dr. Oleg Musin
Chair of Committee

Dr. Alexey Glazryin
Committee Member

Dr. Jacob White
Committee Member

Dr. Jerzy Mogilski
Committee Member

May 2021

ABSTRACT

Sierra, Estefania A., Optimality of Delaunay Triangulations. Master of Science (MS), May, 2021, 44 pp., 3 tables, 38 figures, 19 references.

In this paper, we begin by defining and examining the properties of a Voronoi diagram and extend it to its dual, the Delaunay triangulations. We explore the algorithms that construct such structures. Furthermore, we define several optimal functionals and criterions on the set of all triangulations of points in $\mathbb{R}^d$ that achieve their minimum on the Delaunay triangulation. We found a new result and proved that Delaunay triangulation has lexicographically the least circumradii sequence. We discuss the CircumRadii-Area (CRA) conjecture that the circumradii raised to the power of alpha times the area of the triangulation holds true for all $\alpha \geq 1$. We took it upon ourselves to prove that CRA conjecture is true for $\alpha = 1$, FRV quadrilaterals, and TRV quadrilaterals. Lastly, we demonstrate counterexamples where $\alpha < 1$.

DEDICATION

I am dedicating this thesis to my loving parents, Hermelinda and Alberto Sierra. For their endless love, support, and encouragement throughout all these years in school. Thank you for always telling me that I can achieve anything I set my mind to. For teaching and showing me that education is so valuable and to keep pushing when you feel like things are not going the way they're supposed to. For always motivating me, during all those restless nights and stress where it felt like I was never going to reach the finish line. For encouraging me and giving me the strength I needed when I would question my choice in getting my master's. For always reminding me when I was having a breakdown, that things will align themselves in order they're supposed to happen. For always wanting the best for me. Thank you so much for everything you have done for me.

Dedico esta tesis a mis queridos padres, Hermelinda y Alberto Sierra. Por su amor, apoyo y aliento eterno durante todos estos años en la escuela. Gracias por decirme siempre que puedo lograr cualquier cosa que me proponga. Por enseñarme y mostrarme que la educación es tan valiosa y que debo de seguir empujando cuando se siente que las cosas no van como se suponen que deben de ir. Por motivarme siempre, durante todas esas noches inquietas y estresantes donde sentí que nunca iba a llegar a la meta. Por animarme y darme la fuerza que necesitaba cuando cuestionaba mi elección de conseguir mi maestría. Por recordarme siempre, que las cosas se alinearán en la orden que deben de suceder. Por siempre querer lo mejor para mí. Muchas gracias por todo lo que han hecho por mí.

I also want to thank God for always guiding me towards the right path. For never giving up on me and always listening. Thank you for everything you have helped me accomplished.

I also want to dedicate this thesis to myself as reward for all my hard work throughout these 20 years of school. I just want to say thank you for never giving up on your dreams and pushing past your limits. I'm so proud of you.

ACKNOWLEDGMENTS

First and foremost, I want to thank my parents for instilling in me to always dream big and make those dreams become a reality. Thank you for everything you have given me. I could not have done this without all your love and support.

I want to give a special thanks to Dr. Oleg R. Musin, my advisor and committee chairman, for all the hours he spent helping and guiding me throughout this whole process. Thank you for agreeing to be my advisor during this huge milestone in my journey.

To my committee members who very generously set some time apart from their busy schedules to be part of my thesis committee, I would like to thank you. Thank you Dr. Alexey Glazyrin, Dr. Jacob White, and Dr. Jerzy Mogilski for agreeing to be part of my committee.

I would also like to thank best friends for always understanding and encouraging me when I had moments of doubt. Thank you for all your love. You all mean a lot to me.

I want to give a special thanks to Hugo Gracia for all your love and support throughout this journey. Thank you for always being there for me and motivating me to do my best.

TABLE OF CONTENTS

Page

LIST OF TABLES

Page

LIST OF FIGURES

CHAPTER I

INTRODUCTION

Voronoi diagrams and their dual, Delaunay triangulations, are very important structures in Computational Geometry. That is a reason why their concepts have been rediscovered over time. The properties of both Voronoi diagrams and Delaunay triangulations have been studied by many. Both of these structures have become very powerful tools in a vast variety of areas. As a result, there are several algorithms to compute them. We will discuss in further detail the history and applications of both of these structures in the next few sections.

1.1 History

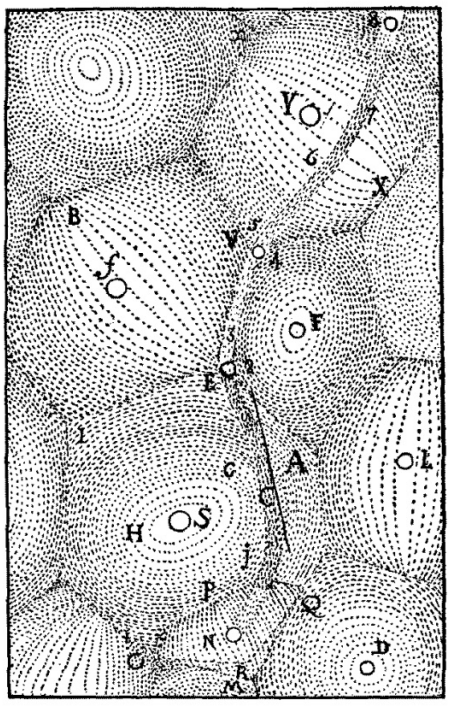

Figure 1.1: Descartes' decomposition of space into vortices.

Even though the Voronoi diagrams were named after Georgy Voronoi, their origins date back to the seventeenth century. René Descartes was one of the first people to mention the concept of Voronoi diagrams [2, 13]. He was a French-born philosopher, mathematician, and scientist. In 1644, Descartes used, what is now known as Voronoi diagrams, to demonstrate that the universe consists of vortices [2, 13]. Descartes claimed that due to the dispersal of matter it created vortices, and fixed stars were the focal element of where the vortices were. Figure 1.1 is an illustration he included in his work, Principles of Philosophy. Now fast forward a few centuries, Johann Peter Gustav Lejeune Dirichlet, a German mathematician was also involved in the study of Voronoi diagrams. In 1850, Dirichlet used Voronoi diagrams for his investigation of positive quadratic forms [2, 13]. Later, Dirichlet's work brought him to the discovery of Voronoi diagrams in two and three dimensions. In 1859, he was able to formalize this idea. Therefore, to this day, Voronoi diagrams are also called Dirichlet tessellations.

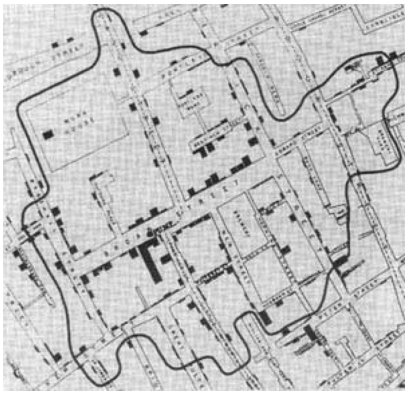

Figure 1.2: Broad street pump

Moreover, in 1854, a serious cholera outbreak in London killed 500 people in five days. John Snow, a physician, gathered statistics on the number of victims and locations of the outbreaks. He divided inner London into neighborhoods, each having a separate water supply [11]. Snow considered the sources of drinking water, and pumps distributed throughout the city. He drew a line labeled "Boundary of equal distance between Broad Street Pump and other Pumps," (refer to Figure 1.2) which basically represented the Broad Street Pump's Voronoi cell [3]. He plotted his data on a chart, effectively constructing a Voronoi diagram. This revealed that almost all fatalities were in

houses supplied by a single pump. When the pump handle was removed, death rates were greatly diminished and the epidemic quickly died out [3, 11]. Snow's work greatly impacted epidemiology.

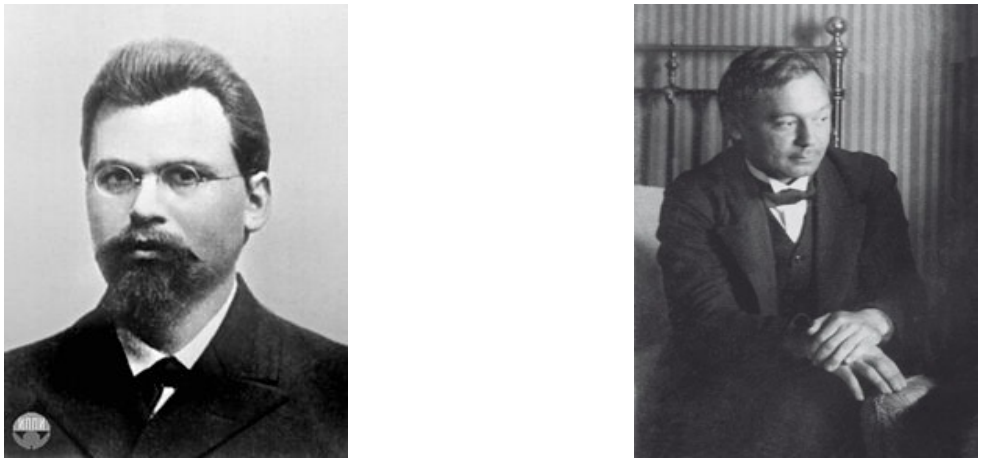

Figure 1.3: Georgy Voronoi and Boris Delone

In 1907, Georgy Voronoi studied the Voronoi diagrams, and extended Dirichlet's work into higher dimensions. Voronoi was able to formalized the general n-dimensional case for Voronoi diagrams [11]. Voronoi also briefly studied the dual diagrams now known as the Delaunay triangulations. However, it wasn't until Boris Delone that Delaunay triangulations were introduced. Boris Delone was intrigued by geometry and started studying previous work on Voronoi diagrams [11]. This led Delone to discover the Delaunay triangulations. Delone generalized Voronoi diagrams and Delaunay triangulations to the case of d-dimensional space [11]. Delone characterized his triangulations through empty circles. This ended up becoming a way used to construct these structures [11].

1.2 Applications

Voronoi diagrams and Delaunay triangulations have many applications. As it can be seen in the history of them, Voronoi diagrams and Delaunay triangulations kept being rediscovered for different purposes. One of the main applications was discussed earlier when John Snow used the Voronoi diagram to single out the pump causing fatalities. This was an application in epidemiology. Voronoi diagrams are also used in computational geometry, robotics, ecology, forestry, geography, zoology, archaeology, and anthropology, just to name a few [6]. For instance, in computational

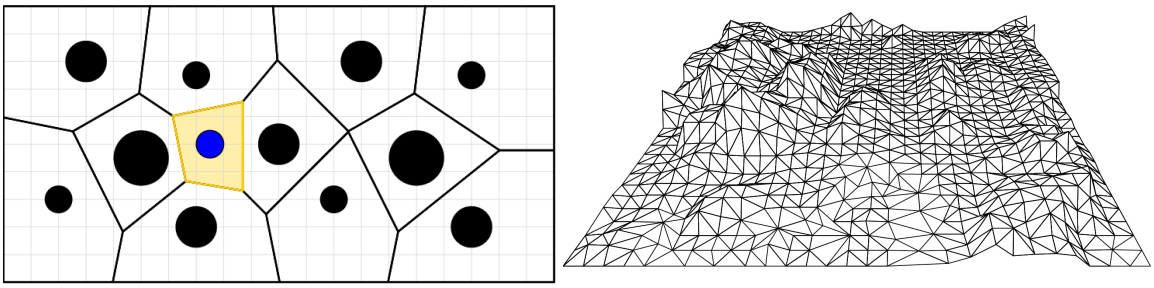

Figure 1.4: Left: Application in robotics [1]. Right: Application in modeling terrain [1].

geometry, Voronoi diagrams are used for representation or quantization problems. Additionally, Voronoi diagrams can also model natural occurrences such as animals' territories or patterns of urban settlements [6]. Moreover, Delaunay triangulations have been used in similar fields as Voronoi diagrams such as computer graphics, robotics, and computational geometry. The Delaunay triangulations have been used to model terrain from physical geography to game development [6]. They can also be used to generate meshes for the finite element method [6]. Overall, the Delaunay triangulations are useful in any area where data represents moving points.

1.3 Introduction

This thesis presents an overview of definitions, properties and algorithms for Voronoi diagrams and their dual, Delaunay triangulations. After getting familiar with their definitions and properties, we will discuss the optimality of various functionals of the Delaunay triangulations. In this thesis, we will present a proof for a conjecture.

To break it down, Chapter II explains the definitions and properties for Voronoi diagrams and Delaunay triangulations. In addtion, it discusses the duality of them and several algorithms that compute these structures. Furthermore, various functionals and criteria that are optimal and achieve their minimum on the Delaunay triangulation are discussed in Chapter III. In this chapter, we provide a proof for Delaunay triangulations having lexicographically the least circumradii sequence see Theorem 3. This leads us to Chapter IV. The goal of this chapter is proving the conjecture of circumradius of a triangulation raised to the power of alpha times the area of a triangulation holds for all $\alpha \geq 1$. This means that it achieves its minimum if and only if t is a Delaunay triangulation.

The conjecture has been proved for $\alpha = 2$ in [7]. We will consider the case of $\alpha \geq 1$ is true for this conjecture. Now, the last chapter is for the conclusion of this paper. We will summarize everything that was done in this thesis and the remaining properties left to be proved.

CHAPTER II

VORONOI DIAGRAMS AND DELAUNAY TRIANGULATIONS

2.1 Definitions, Properties, and Algorithms of Voronoi Diagrams

A Voronoi diagram is a collection of regions that divide up the plane. Each region corresponds to one of the sites (points), and all the sites in one region are closer to the corresponding site than to any other site [19]. This would be considered an informal definition. We will accurately define it later in the chapter. However, this brief definition helps grasp the main idea of what it is. Now, for instance, let's take a look at the post office problem. Let's say there are several post offices in the city. In Figure 2.1(a), consider the sites to be the locations of the post offices in the city.

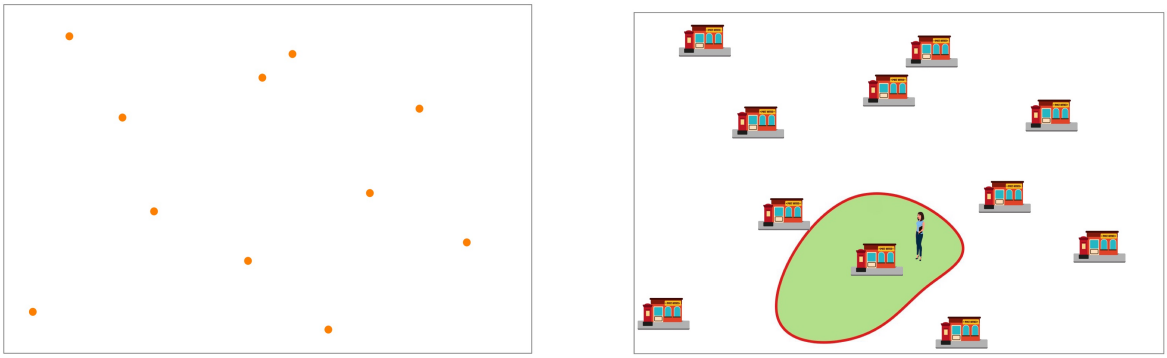

(a) Voronoi Sites (b) Voronoi Sites as Post Offices

Figure 2.1: Post office problem

How can we determine which post office is closest to us? To figure this out, we would have to analyze the whole map and for every site, we would have to find out which is the closest post office to it. Therefore, we can divide the map into regions where every region knows which is the closest post office [19]. After that, all you need to know is which region you are in to find the closest post office. Let's analyze the simplest example to demonstrate what occurs at every site. As it can

be seen in the Figure 2.2, there are two sites p and q. We would have to take the bisection of the two sites. In order to do that, we consider the line segment connecting the two sites and take the perpendicular bisector. The perpendicular bisector passes through the midpoint of the line segment pq and is perpendicular to it. Thus, if you are on the right section, then the closest post office is q. If you are the left section, then the closest post office is p.

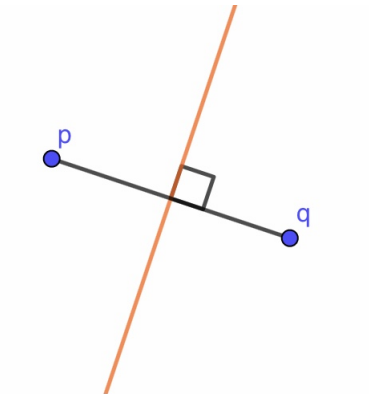

Figure 2.2: The bisection of two sites

2.1.1 Definitions and Properties

Let's consider the points p and q. Denote the bisection of p and q as $b(p,q)$ and their Euclidean distance as $d(p,x)$ [2]. Then, it's bisection can be defined as

$$b(p,q) = \{x \in R^2 : d(p,x) = d(q,x)\}.$$

This means that the distance to p is the same as the distance to q hence it's on the perpendicular bisector (orange line). On the left section, we have the half plane that is closer to p than q [2]. This can be defined as

$$h(p,q) = \{x : d(p,x) < d(q,x)\}.$$

On the right section, we have the half plane that is closer to q than p and its defined as

$$h(q,p) = \{x : d(q,x) < d(p,x)\}.$$

However, what if we have more than two sites. Figure 2.3 demonstrates how the Voronoi diagram would look like.

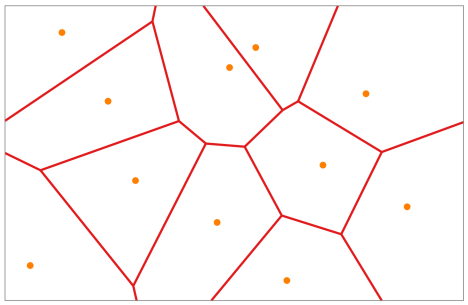

Figure 2.3: $Vor(P) =$ Voronoi diagram of P

Now let's take a look into the formal definition of a Voronoi diagram.

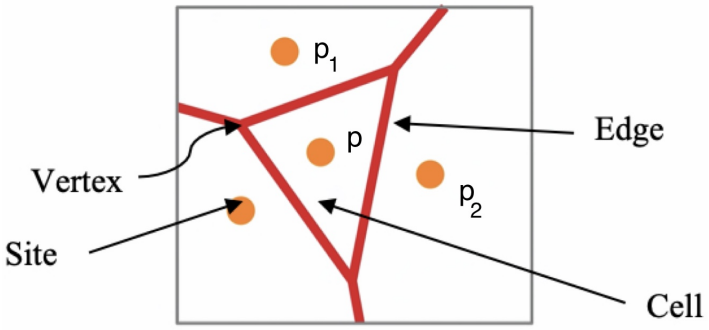

Figure 2.4: Voronoi diagram of 4 points

Definition 1. ***(Voronoi Cell)*** *Let P be a set of points in $\mathbb{R}^d$. Then the Voronoi cell V_c of $p \in P$ is defined as*

$$V_c = \{x \in \mathbb{R}^d : d(p,x) \leq d(q,x) \ \ for\ all \ \ q \in P\}.$$

The Voronoi cell is defined as the set of all points in $\mathbb{R}^d$ that are closer to p than they are to any other point q. This means the distance to p is smaller than the distance to all other points of this set [2, 19]. This always exist for every point so at least the point itself has to lie on its own Voronoi cell. Thus, it cannot be empty.

Proposition 1.

$$V_c = \cap_{q \neq p} h(p,q)$$

The Voronoi cell can be defined similarly as the two point case. Previously, we had shown that we need the bisector between two points and that gives us the region of the cell of each of these points. Now, if we do the same for all pairs of points, then we find the half plane that is closer to p then to another point q [2, 19]. This is defined by all the points that lie on its side of the bisection. Now, if we intersect all of these then we get the cell. If a point lies inside the half plane, then it's closer to p then to any other point.

Definition 2. *Let P be a set of points in $\mathbb{R}^d$ and let $p, p_1, p_2 \in P$. Then the Voronoi edge V_e is defined as*

$$V_e = \{x : d(p,x) = d(p_1,x) \ \ and \ \ d(p,x) < d(q,x) \ \ \forall q \neq p, p_1\}$$

The Voronoi edge is defined by two points. Using Figure 2.4, there is an edge between the Voronoi cell p and the Voronoi cell p_1. These points have the same distance to the edge but there is also no other point that is closer to it.

Definition 3. *Let P be a set of points in $\mathbb{R}^d$ and let $p, p_1, p_2 \in P$. Then the Voronoi vertex V_v is defined as*

$$V_v = \{x : d(p,x) = d(p_1,x) = d(p_2,x) \ \ and \ \ d(p,x) \leq d(q,x) \ \ \forall q\}$$

The Voronoi vertex is defined by three points p, p_1, p_2. This is the boundary of the Voronoi cell where p, p_1, p_2 meet so this point has three closest points in the point set. p, p_1, p_2 have the same distance from the vertex [2, 19]. Therefore, we can define it similarly as the Voronoi edge, but this time with three points instead of two. However, the difference is that a Voronoi vertex can have three or more points with the same distance.

Definition 4. *Voronoi diagram of P is defined by*

$$Vor(P) = \cup_{p \neq q} V_c(p,P) \cap V_c(q,P)$$

Lemma 1. *Let P be a set of points in a plane. We can say $Vor(P)$ is composed of $n-1$ parallel lines if all the points are collinear. If not, $Vor(P)$ is connected and its edges are line segments of half lines.*

Proof. Let's assume that P is not collinear. Suppose that there is an edge e that is a full line in $Vor(P)$ where edge e is the bisection of p and q.

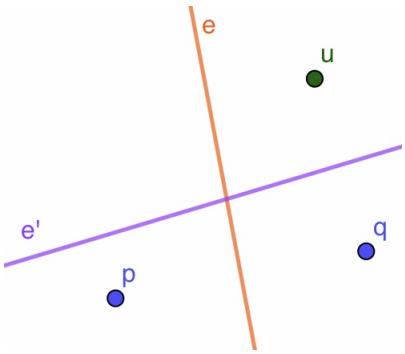

Figure 2.5: Proof of lemma 1

Now, let u be a point in P that is not collinear with p and q. Let e' be the bisection of u and q. Then, e' is not parallel to e. Therefore, e' intersects e. However, the section of e that is on the half plane that is closer to u than to q forms a contradiction because e is bounded to at least one side. □

The proof of Lemma 1 was shown using the references [2, 19].

Lemma 2. *Given a set P of n sites, $Vor(P)$ consists of at most $2n-5$ vertices and $3n-6$ edges.*

Proof. Using Euler's formula where $f =$ faces, $v =$ vertices, and $e =$ edges.

$$f = n \Rightarrow (v+1) - e + n = 2$$

Since the minimum is 3 vertices and 2 edges, then

$$2e \geq 3(v+1)$$

$$e \leq \frac{3}{2}(v+1)$$

Thus, we get

$$(v+1) - \frac{3}{2}(v+1) + n \leq 2$$

$$\frac{1}{2}(v+1) \leq n-2$$

$$v \leq 2n-5$$

Similarly, the edges can be derived from above. Hence, there are $3n-6$ edges and $2n-5$ vertices.

□

The proof of Lemma 2 was shown using the references [2, 16, 19].

Lemma 3. *For the Voronoi diagram $Vor(P)$ of a set of points P and $C_P(x)$, the largest empty circle centered at x, the following holds [2, 19]:*

1. *A point x is a vertex of $Vor(P)$ if and only if $C_P(x)$ contains three or more sites on its boundary.*
2. *The bisector between sites p and p_1 defines an edge of $Vor(P)$ if and only if there is a point x on the bisector such that $C_P(x)$ contains both p and p_1 on its boundary but no other site.*

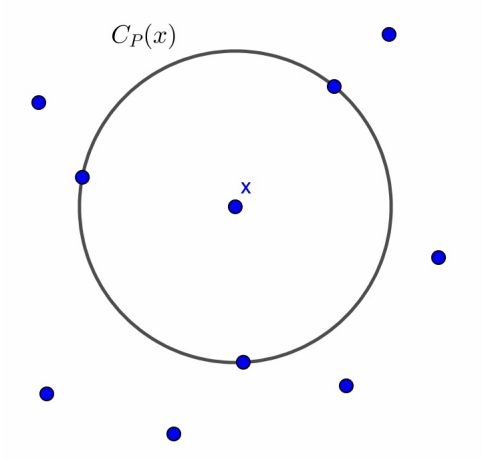

Figure 2.6: The largest empty circle centered at x.

Lemma 4. *A point p of P lies on the convex hull of P if and only if its Voronoi cell V_c is unbounded.*

The proof for this lemma will not be shown, but can be found in the following references [2, 19].

2.1.2 Algorithms

In addition, there are algorithms that help construct the Voronoi diagrams. The first one is called the Half Plane Intersection algorithm. This algorithm is not the best one to construct the Voronoi diagrams. This process takes $O(n^2 logn)$ time which means it is not the fastest way to create a Voronoi diagram [19]. However, later in the chapter we will discuss a faster method to construct one.

The steps to construct a Voronoi diagram using the Half Plane Intersection algorithm are the following:

1. Take the perpendicular bisector of two neighboring sites (see Figure 2.7a). The perpendicular bisector becomes the Voronoi edge.

2. Repeat step 1 for all neighboring sites.

3. Construct a circle passing through 3 neighboring sites. The center of the circle becomes the Voronoi vertex. As can be seen in Figure 2.7d, the vertices are in green.

4. The Voronoi cell is now complete. This process is repeated for every site to build the entire Voronoi diagram (see the Voronoi cell for site B in Figure 2.7c).

Furthermore, in 1986, Steven Fortune created the sweep line algorithm. It was used to generate Voronoi diagrams in $O(nlogn)$ time and $O(n)$ space. The Fortune's algorithm takes a sweep-line approach. It is a horizontal line moving from top to bottom where the sites above the line have been added to the Voronoi diagram and the sites below the line have not yet been considered. This algorithm also includes a x-monotone curve which is called the beach line which follows the sweep line as it moves down [19]. It is called the beach line because the curved line looks like beach waves. However, they are just parabolic arcs forming around the site as the sweep line moves. This

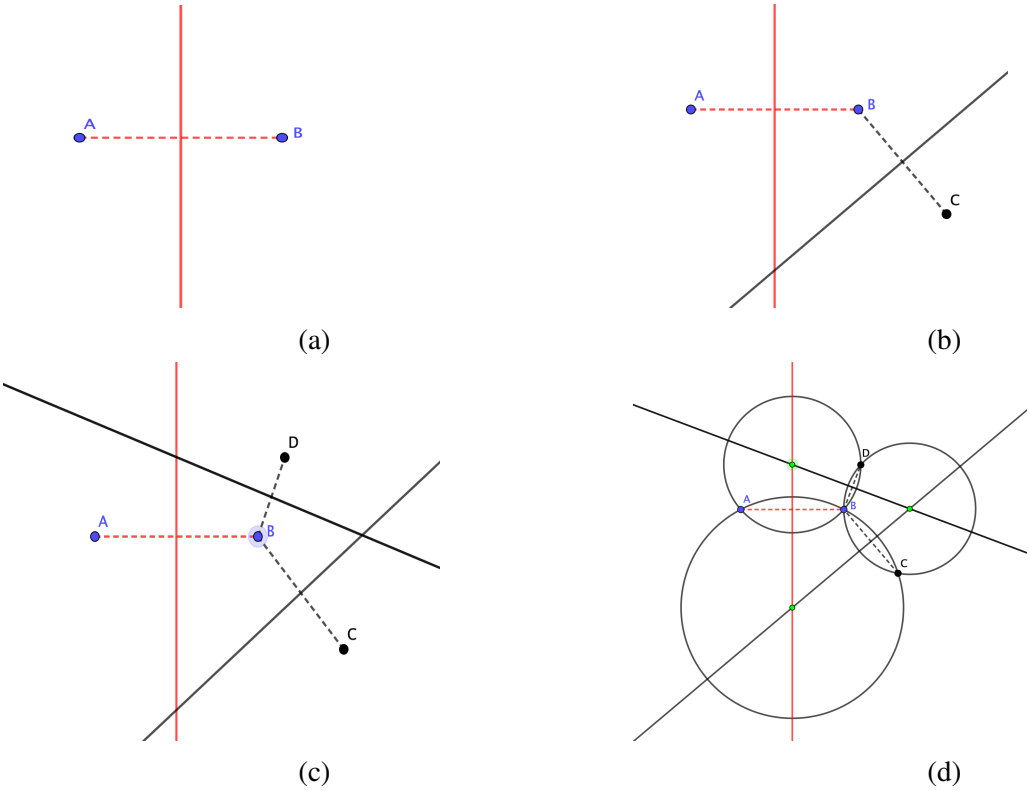

Figure 2.7: Half plane intersection algorithm

is done by using the sweep line as the directrix and the site as the focus. Therefore, every point on the parabolic curve is equidistant to p and L as can be seen in Figure 2.8. Moreover, the breakpoints of the beachline trace out the Voronoi edges [19]. New arcs on the beachline only appear through site events, that is, whenever the sweep line hits a new site. This means that we have at most $2n - 1$ arcs at the same time [19]. This is because the first site gives us exactly one and every new one can split an old arc into two parts. Thus, we can get two more every site we encounter.

There are two events that can occur in this algorithm. The first one being the site event as previously mentioned. The site event occurs as the sweep line moves downwards it will sweep over new sites. This in exchange will add a new parabola into the beach line [19]. Now, the second event that can occur is called the vertex event. This happens when the length of a parabolic arc keeps shrinking until it disappears and a new Voronoi vertex will be created at this point [19].

For the vertex event, it occurs when the sweep line reaches the lowest point of a circle. There are three sites above the sweep line, and the center of the circle is equidistant from all three sites

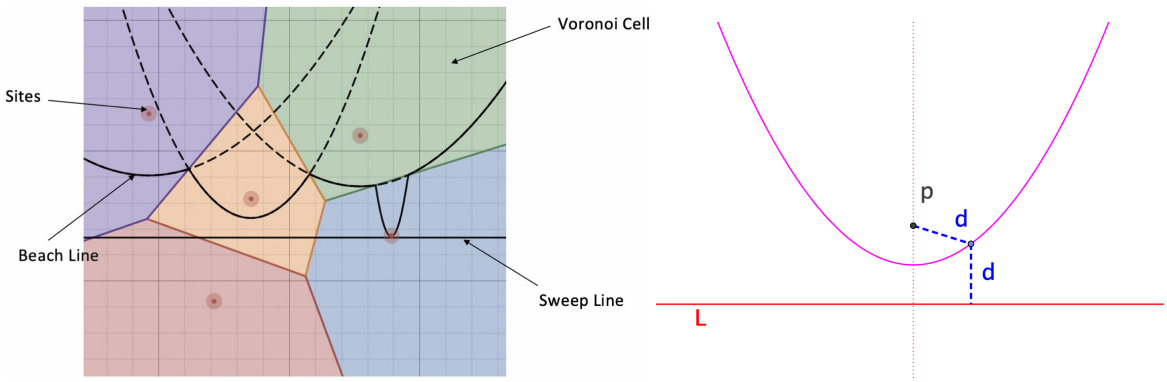

Figure 2.8: Left: Fortune's algorithm. Right: Parabolic arcs forming.

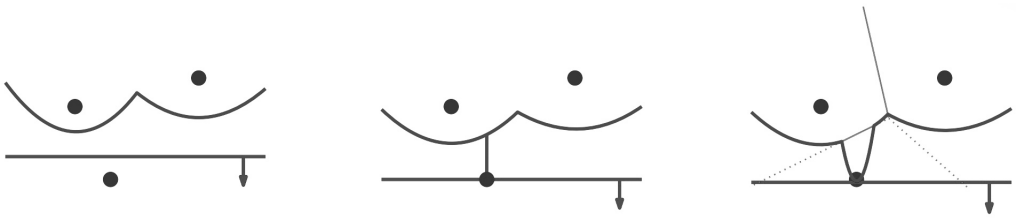

Figure 2.9: Site event [19]

and from the sweep line. The parabolic arcs are consecutive on the beachline. Thus, when there is a vertex event, a parabolic arc disappears from the beach line, and the center of the circle becomes the vertex of the Voronoi diagram [19]. Furthermore, arcs only disappear from the beachline at vertex events.

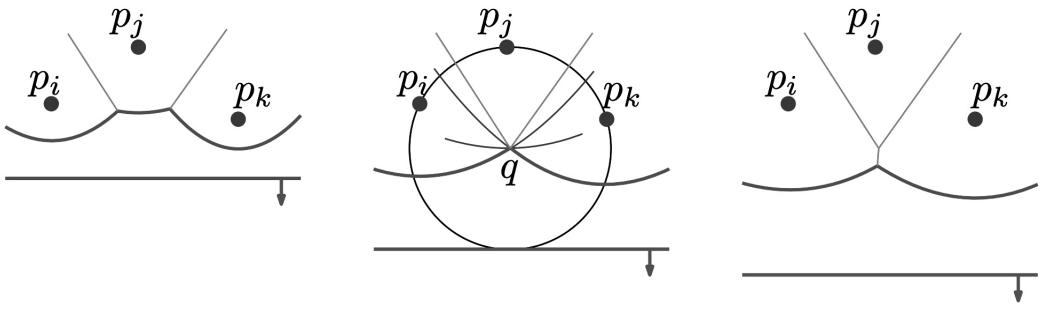

Figure 2.10: Vertex event [19]

2.2 Duality

In section 2.1, we discussed what Voronoi diagrams are and their respected properties. We will now consider a related structure called the Delaunay triangulation (DT), which is the dual to the

Voronoi diagram. Delaunay triangulations are triangulations that are formed from the connection of the site points of a Voronoi diagram. The Voronoi vertices are the centers of the circumcircles, a circle passing through all the vertices of a triangle. There are no points that will lie inside the circumcircle of a triangle.

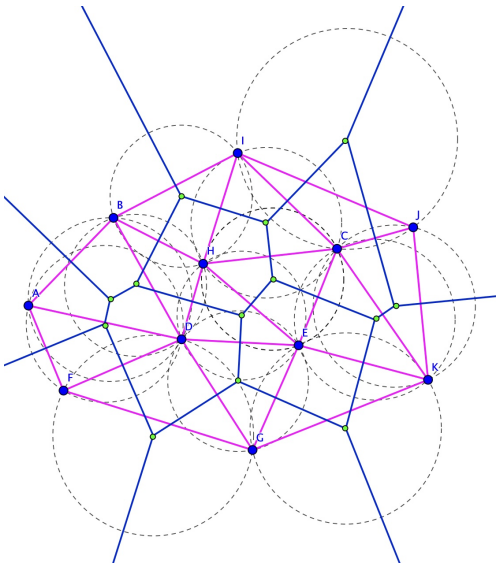

Figure 2.11: Voronoi diagram and its dual Delaunay triangulation

Due to the duality of the graphs, the properties of the Delaunay triangulation results from the structure of the Voronoi diagram. For instance, the convex hull of the Delaunay triangulation is the boundary of the exterior sites of the Voronoi diagram. The circumcircle property is also an immediate result from the Voronoi diagram. The circumcircle of any triangle in the Delaunay triangulation is considered empty because the interior of the circle contains no sites (see the dotted circle in Figure 2.11). Since in its dual structure, the center of the circle is the vertex in the Voronoi diagram as seen in Figure 2.11. Moreover, the empty circle property will be discussed further later in the chapter.

Formally, from our Voronoi diagram the dual graph is defined as follows.

Definition 5. *The graph $G = (P,E)$ with $\{p,q\} \in E \iff V_c(p)$ and $V_c(q)$ share an edge. Then the graph G is the dual graph of $Vor(P)$.*

The vertex set of this graph is the point set P. In the Voronoi diagram there is one Voronoi

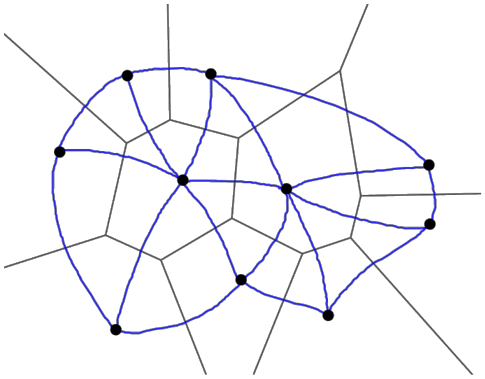

Figure 2.12: Graph G = dual graph of $Vor(P)$

cell for every site (point). However, here the sites are the vertices of the dual graph. Then, in this graph, we have an edge between two vertices of the Voronoi diagram. Now, the dual graph of $Vor(P)$ is to take all the sites and connect them if the corresponding Voronoi cells share an edge [19].

Definition 6. *The Delaunay graph $DG(P)$ is the straight line drawing of G.*

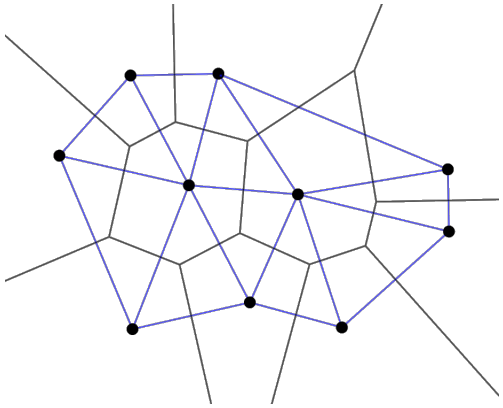

Figure 2.13: Delaunay graph

The Delaunay graph is taking the dual graph and draw all these edges in Figure 2.12 as straight line segments [19]. Note that the Delaunay graph doesn't have to be a triangulation. Instead, we will call all triangulations Delaunay if they contain the Delaunay graph as a subgraph.

2.3 Definitions, Properties, and Algorithms of Delaunay Triangulations

Delaunay triangulations can be useful in many fields. Since we have informally defined what Delaunay triangulations are in the previous section. Let's consider height interpolation. Let's say we have a topographic map and we want to show, for all the points, what is the height of the point and how far above absolute zero it is. In order to do that, we have to measure the height for every single point in the map. Since that would be way too much, we instead only measure the height at some points and interpolate for everything in between. Using the sample points, we can project them onto a plane. Since we still need to figure it out for all the points in between, then we have to interpolate them. For interpolating, we just want to look at a few close points for the section we want to interpolate. Thus, we use a triangulation of the point set to interpolate. Moreover, for every edge, we have to interpolate between the two points that it connects, and for each triangle in the triangulation, we only have to interpolate between the three points that construct the triangle. Finally, we can lift each sample point to its correct height, and we have a good approximation.

2.3.1 Definitions and Properties

Before we can define the Delaunay triangulation, let's first define a triangulation.

Definition 7. *A triangulation of P is a maximal planar graph with vertex set P, that is, no edge can be added without crossing other edges.*

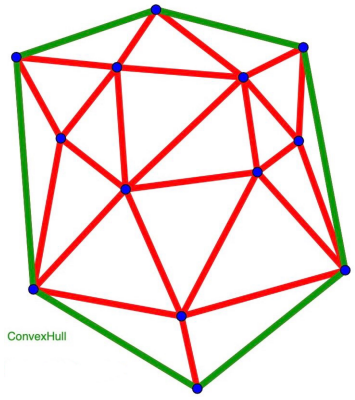

Figure 2.14: The convex hull is the boundary of the triangulations.

The following are properties of a triangulation [4, 19]:

1. A triangulation is made of triangles hence the internal faces are triangles.

2. The outer polygon is a convex hull, that is, each triangulation of P contains the edges of the convex hull of P, $CH(P)$.

Lemma 5. *Let P be a set of n sites, not all collinear, and let h be the number of sites on $\partial CH(P)$. Then any triangulation of P has $2n-2-h$ triangles and $3n-3-h$ edges.*

This lemma can be proved by using Euler's formula [12, 19]. However, this lemma only works for $\mathbb{R}^2$. For d-dimensional, the number of simplices ranges from $O(n)$ to $O(n^{\frac{d}{2}})$.

Now that we know what a triangulation and a Delaunay graph is, we can start defining a Delaunay triangulation.

Lemma 6. *Let P be a set of points in the plane. Then*

1. *There are points $p_1, p_2, p_3 \in P$ which are the vertices of the same face of the $DG(P)$ if and only if the circle through the three points does not contain a point of P in its interior.*

2. *There are points $p_1, p_2 \in P$ that form an edge of the $DG(P)$ if and only if there is a closed circle C that contains p_1 and p_2 on its boundary and no other point of P.*

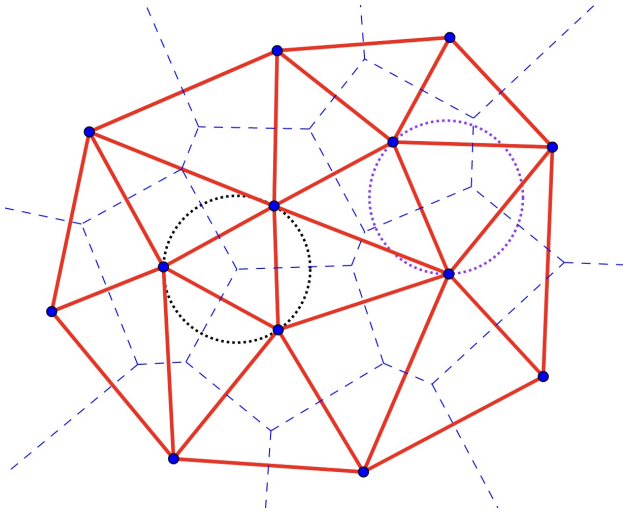

Figure 2.15: Circumcircle property

This lemma describes the circumcircle property. Since the center of the circle that contains points p_1, p_2, and p_3 is the corresponding vertex of the Voronoi diagram. Thus, by Definition 3, the three points are the nearest neighbors to that Voronoi vertex (see black circle in Figure 2.15) [2, 4, 12, 19]. Moreover, part 2 can be proved by contradiction by assuming that the triangulation formed by p_1, p_2, and p_3 is not Delaunay. Therefore, there lies a point inside the circumcircle. So, when we try to find an empty circle that passes through the edge, there will be a point of P that lies inside. Thus, it cannot be a Delaunay edge since there is no empty circle for edges [2, 4, 12, 19].

Now that we know how to get the Delaunay triangulation from the Delaunay graph, let's consider the empty circle property. We need to know how this property works to fully understand Lemma 6.

Let p_1, p_2, p_3 be a triangulation of a set of points. Then, the triangulation p_1, p_2, p_3 is a Delaunay triangulation if and only if its circumcircle does not contain any other points besides the points in the triangulation. If the triangulation satisfies the empty circle test, then it is a Delaunay triangulation [19]. In the rejected Figure 2.16, we can see that it does not satisfy the empty circle test [12]. That is because point p_2 lies inside the circle thus it cannot be a Delaunay triangulation. However, in the accepted Figure 2.16, we see that the circumcircle is empty [12]. This means none of the other points lie inside the circle.

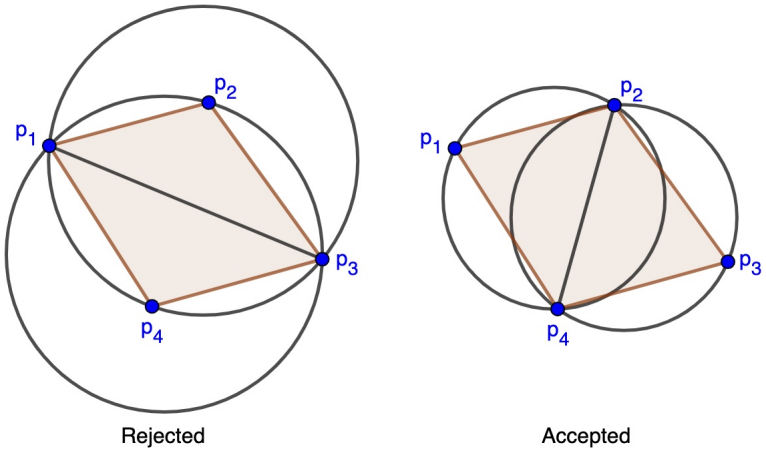

Figure 2.16: Empty circle test

Theorem 1 (Delaunay, 1934)**.** *Let P be the triangulation of points. If P satisfies the Empty Circle*

Test, then it is a Delaunay triangulation.

Boris Nikolaevich Delaunay proved this theorem in 1934. It can be found in [5].

Lemma 7. *Given a set $P \subset \mathbb{R}^2$ of four points that are in convex position but not cocircular. Then P has exactly one Delaunay triangulation.*

In [8], the proof for lemma 7 can be found.

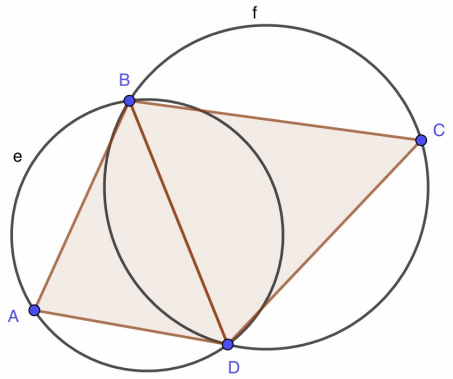

Figure 2.17: Case of four points

Given a triangulation of P, we call an edge locally Delaunay if it passes the empty circle test.

Lemma 8 (Delaunay, 1934)**.** *If the edge of a triangulation t of P is locally Delaunay then t is $DT(P)$.*

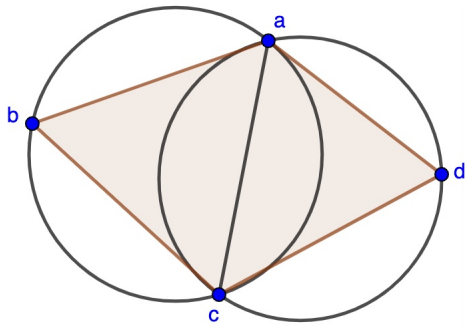

Figure 2.18: Locally Delaunay

Furthermore, let's suppose that an edge *ac* is shared by the triangles *abc* and *adc*. If the triangle *abc* satisfies the empty circle property, then the point *d* will lies outside the circumcircle of triangle *abc*. Thus, the edge *ac* is called legal and locally Delaunay. In addition, this property is symmetrical. Therefore, *b* is outside the circumcircle of triangle *adc*. Now, an edge *ac* is called illegal and not locally Delaunay if *d* is inside the circumcircle of triangle *abc*, and once again, this property is symmetrical [2, 19]. This means that *b* will lie inside the circumcircle of triangle of *adc* as well. This brings us to the edge flipping property. If we have an edge that is not locally Delaunay, we can flip it with the other diagonal in the convex quadrilateral. This operation states that if you flip an edge that is not locally Delaunay, then the new edge is locally Delaunay. Moreover, if it is a concave quadrilateral, then flipping the edge leads to an invalid configuration with two overlapping triangles. Now if all the edges are locally Delaunay, then the triangulation is a Delaunay triangulation [4]. So, let's suppose we can start with an arbitrary triangulation. We can convert it to a Delaunay triangulation by flipping all the illegal edges and making them legal [4, 19].

2.3.2 Algorithm

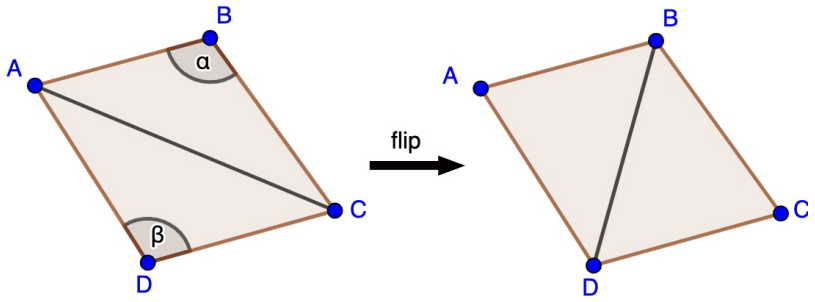

Figure 2.19: Flip algorithm

This leads us to the Flip Algorithm. This algorithm starts with the construction of an arbitrary triangulation of a point set P. When two triangles form a convex quadrilateral *ABCD*, the shared diagonal *AC* is flipped if and only if the angles $\alpha + \beta > 180^\circ$ and replaced by diagonal *BD* [19]. The edges get flipped until no triangle is non-Delaunay [4]. If we cannot do more flips then the triangulation is *DT*. The Flip Algorithm follows Lemma 8. This algorithm takes $O(n^2)$ edge flips which makes it a simple one to use.

CHAPTER III

OPTIMALITY OF DELAUNAY TRIANGULATIONS

There are several functionals and criteria that optimize the Delaunay triangulation. We will discuss them in the next two sections. Lastly but most importantly, we will discuss the Circumradii Area conjecture and what is needed to show its optimal in the Delauny triangulation.

3.1 Optimal Criteria

3.1.1 Max-Min Angle Criterion

The diagonal of every convex quadrilateral that happens in a triangulation can be replaced by another diagonal if the alternative one does not increase the minimum of the six angles in the two triangles making up the quadrilateral [10, 15, 18]. Thus, the Delaunay triangulation maximizes the minimum angle in a triangle. This means that the Delaunay triangulation stays away from "skinny" triangles [12].

3.1.2 Lexicographical Angle Sequence

Moreover, a Delaunay triangulation maximizes the smallest angle, the second smallest angle, the third smallest angle and so on. This can be associated with the angle sequence. This is defined as the increasing sequence of angles $(\theta_1, \theta_2, ..., \theta_m)$ that appear in the triangles. Furthermore, this is the first theorem about optimal properties of Delaunay triangulation, and it was proved in 1978 by Sibson [18].

Theorem 2. *Among all triangulations of a given point set, the Delaunay triangulation has the lexicographically largest angle sequence.*

Proof. Let's begin the proof by recalling the inscribed angle theorem. This theorem states that the

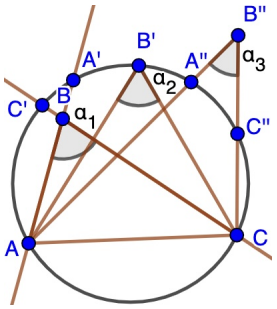

Figure 3.1: Angles

measure of an inscribed angle is half the measure of the intercepted arc. Since, in our case we are looking at an inscribed triangle, then each angle will be half the measure of the minor arc. Now, the interior angle is the average of the minor arc and the arc that forms when the lines intersecting at B get extended (see Figure 3.1). On the other hand, the exterior angle is half the difference between the minor arc and the intercepted angle formed as B'' extends outside the circle.

$$a_1 = \frac{1}{2}(\overset{\frown}{AC} + \overset{\frown}{C'A'})$$
$$a_2 = \frac{1}{2}(\overset{\frown}{AC})$$
$$a_3 = \frac{1}{2}(\overset{\frown}{AC} - \overset{\frown}{A''C''})$$

Thus, we can see from Figure 3.1 and the definitions that $a_1 > a_2 > a_3$.

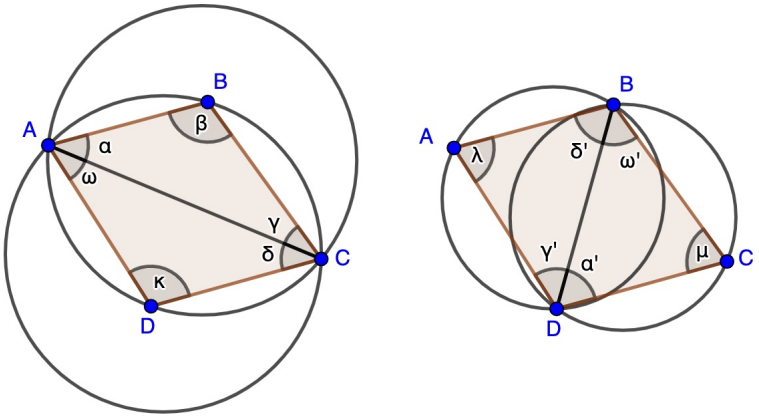

Figure 3.2: Edge flips

Let $ABCD$ be a convex quadrilateral. Then, we have two adjacent triangles ΔABC with

angles $\angle\alpha, \angle\beta, \angle\gamma$ and ΔADC with angles $\angle\delta, \angle\kappa, \angle\omega$ (see Figure 3.2).

Suppose that ΔABC and ΔADC fails to satisfy the empty circle property resulting in ΔABC and ΔADC being non-Delaunay. Therefore, we do an edge flip where the diagonal AC is replaced by BD. The empty circle property is satisfied by ΔABD and ΔBCD. Thus, it is a Delaunay triangulation.

Hence, we have

$$\angle\alpha' > \angle\alpha, \quad \angle\gamma' > \angle\gamma$$

$$\angle\delta' > \angle\delta, \quad \angle\omega' > \angle\omega.$$

This is proved by using the observation from Figure 3.1 and its definitions at the beginning.

In the orginal triangulations, we have $\angle\beta$ and $\angle\kappa$. Since we did the edge flip, we now have $\angle\lambda$ and $\angle\mu$. However, these angles cannot be smaller than the minimum of $\angle\alpha, \angle\gamma, \angle\delta, \angle\omega$. Thus, DT has lexicographically the largest angle sequence. □

3.1.3 Lexicographical Circumradii Sequence

Not only that, but it also applies to the sequence of radii of the circumcircles of the Delaunay triangulation. The circumradii is the smallest when the triangulation is DT.

Let t be a triangulation of P and let Δ be a triangle in t. Let $R(\Delta_1), R(\Delta_2), ..., R(\Delta_m)$ be the circumradii of triangles in t in increasing order such that $R(\Delta_1) \leq R(\Delta_2) \leq ... \leq R(\Delta_m)$. We call this the circumradii sequence of t.

Theorem 3. *Among all triangulations of a given point set, the Delaunay triangulation has the lexicographically least circumradii sequence.*

Proof. Suppose we have a convex quadrilateral $ABCD$ with two triangulations $(\Delta ABD, \Delta BCD)$ that share an edge BD and $(\Delta ABC, \Delta ADC)$ that share an edge AC. Denote $R_A = R(\Delta ABD), R_B = R(\Delta ABC), R_C = R(\Delta BCD), R_D = R(\Delta ADC)$ as the circumradius.

Let

$$R_A \leq \min(R_B, R_C, R_D)$$

Theorem 9 from section 4.2 states that $t_{BD} = \{\Delta ABD, \Delta BCD\}$ is DT and we have one of two cases:

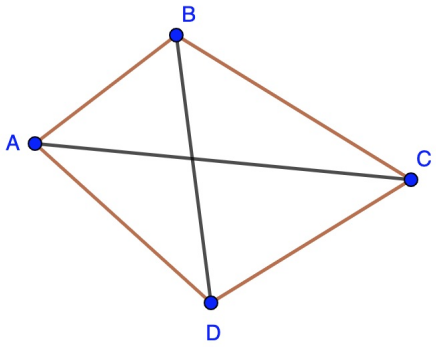

Figure 3.3: *ABCD*

1. $R_A \leq R_C \leq R_B \leq R_D$ or

2. $R_A \leq R_B \leq R_C \leq R_D$

It is easy to see that (R_A, R_C) is lexicographically less than (R_B, R_D). □

3.1.4 The Radii Criterion

This criterion is the mean of circumradii of triangles in $\mathbb{R}^2$. In [15], Musin states that a triangulation that contains "minimal sum of radii" is of greater quality since its triangulations are closer to being regular triangles.

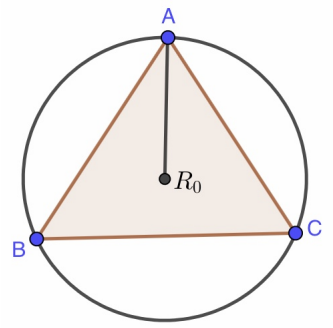

Figure 3.4: Circumcircle radius

Let t be a triangulation of P in $\mathbb{R}^2$ and let Δ be a triangle in t. Then we define

$$R_a(\Delta) = R_0^a, \text{ where } R_0 \text{ is the circumcircle radius.}$$

Let $\Delta_i \in t$. Then we define

$$R_a(t) = \sum_{i=1}^{m} R^a(\Delta_i), \text{ where } m \text{ is the number of triangles in } t \text{ and } a > 0.$$

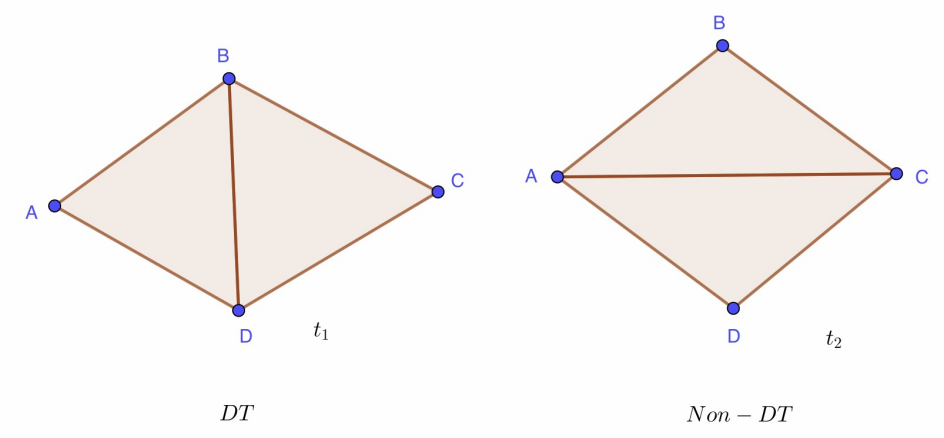

Figure 3.5: Example of DT and non-DT

The following theorem easily follows from Theorem 3.

Theorem 4. *$R_a(t)$ achieves its minimum if and only if t is DT(P).*

3.1.5 The Inradii Criterion

Lambert demonstrated that the Delaunay triangulation maximizes the mean inradii of triangles.

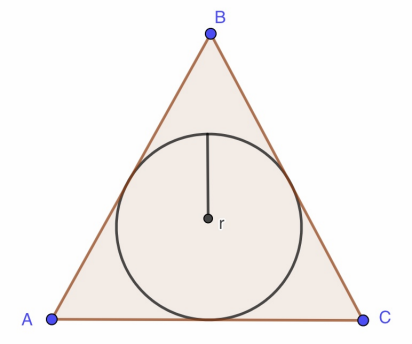

Figure 3.6: Inradius of ΔABC

Let t be a triangulation of P in $\mathbb{R}^2$ and let Δ be a triangle in t. Then we define

$$r(\Delta) = \text{ the inradius of } \Delta$$

Let Δ_i be a set of triangles in t. Then we define

$$r(t) = \sum_i r(\Delta_i)$$

Theorem 5 (Lambert, 1994)**.** *The functional $r(t)$ attains its maximum if and only if t is $DT(P)$.*

The proof of this theorem can be found in [9].

3.2 Optimal Functionals

3.2.1 The Harmonic Index

Suppose there is a polygon Δ (see Figure 3.7), then its harmonic index ($hrm(\Delta)$) is the sum of squares of lengths of the sides of Δ divided by the area of Δ.

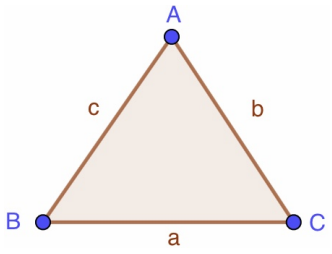

Figure 3.7: Polygon Δ

Let t be a triangulation of P in $\mathbb{R}^2$ and let Δ be a triangle in t. Then we define the harmonic index as

$$hrm(\Delta) = \frac{a^2+b^2+c^2}{Area(\Delta)}, \text{ where } a,b,c \text{ are the sides of polygon } \Delta.$$

Let $\Delta_i \in t$. Then we define

$$hrm(t) = \sum_{\Delta_i \in t} hrm(\Delta_i)$$

Theorem 6 (Musin,1995)**.** *The harmonic index $hrm(t)$ of a triangulation t of P achieves its minimum if and only if t is $DT(P)$.*

The proof for the harmonic index can be found [15]. Musin used the theorem of Local Circle Test (LCT) to show that it was minimal which the proof for LCT can also be found in [15].

3.2.2 Weighted Sum of Squares of the Edge Lengths

Rajan [17] proved that the weighted sum of squares of the edge lengths is the smallest for Delaunay triangulation, where the weight is the sum of volumes of the triangles incident on the edge.

Let t be a triangulation of P in $\mathbb{R}^2$ and let Δ be a triangle in t. Then we define

$$E(\Delta) = (a^2 + b^2 + c^2) \cdot Area(\Delta)$$

Let $\Delta_i \in t$. Then we define

$$E(t) = \sum_i E(\Delta_i)$$

Theorem 7 (Rajan, 1994)**.** *$E(t)$ achieves its minimum if and only if t is the $DT(P)$.*

3.2.3 Voronoi Functional

Let t be a triangulation of P in $\mathbb{R}^2$ and let Δ be a triangle in t. Then we define the Voronoi functional as

$$Vf(\Delta) = area(\Delta)(a^2 + b^2 + c^2 - 4R^2)$$

This was proved in [7]. This functional $Vf(t)$ achieves its maximum if and only if t is $DT(P)$.

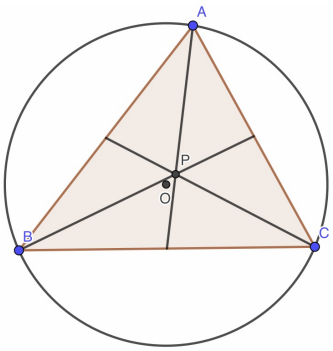

Figure 3.8: Centroid and circumcenter

3.2.4 D Functional

Let P be the centroid and O the circumcenter of a triangle $\Delta \in t$ where t is a triangulation in P in $\mathbb{R}^2$ (see Figure 3.8). Then we define

$$D(\Delta) = ||centroid(\Delta) - circumcenter(\Delta)||^2 \cdot Area(\Delta)$$

Let $\Delta_i \in t$. Then we define

$$D(t) = \sum_{i=1}^{m} D(\Delta_i), \text{ where } m \text{ is the number of triangles in } t.$$

Conjecture (Musin, 2010): *$D(t)$ achieves its minimum if and only if t is $DT(P)$.*

3.3 CircumRadii-Areas (CRA)–Conjecture

Let t be a triangulation of P and let Δ be a triangle in t. Then we define

$$R_\alpha(\Delta) = R^\alpha(\Delta) \cdot Area(\Delta), \text{ where } R^\alpha(\Delta) \text{ is the circumradius of } \Delta.$$

$$R_\alpha(t) = \sum R^\alpha(\Delta_i) \cdot Area(\Delta_i)$$

Conjecture: *If $\alpha \geq 1$, then $R_\alpha(t)$ achieves its minimum if and only if t is $DT(P)$.*

This conjecture is proved for $\alpha = 2$ in [7]. We are going to consider this conjecture for all $\alpha \geq 1$.

CHAPTER IV

CRA–CONJECTURE ON DELAUNAY TRIANGULATION

Notations:

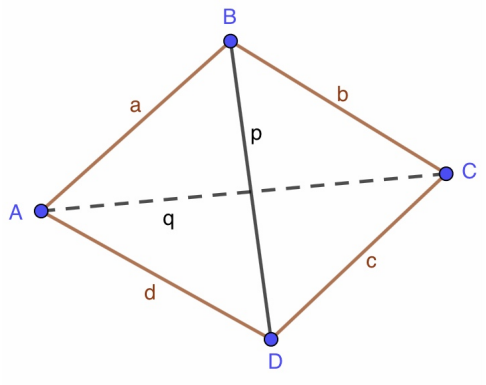

Figure 4.1: ABCD

$R_A = R(\Delta ABD)$

$R_B = R(\Delta ABC)$

$R_C = R(\Delta BCD)$

$R_D = R(\Delta ADC)$

$S_A = Area(\Delta ABD)$

$S_B = Area(\Delta ABC)$

$S_C = Area(\Delta BCD)$

$S_D = Area(\Delta ADC)$

$t_{BD} = \{\Delta ABD, \Delta BCD\}$

$t_{AC} = \{\Delta ABC, \Delta ACD\}$

$a = |AB|, b = |BC|, c = |CD|, d = |DA|$ $p = |BD|$, $q = |AC|$.

$|XY|$ denote the Euclidean distance between X and Y.

4.1 CRA–conjecture for a quadrilateral

In section 3.3, we define

$$R_\alpha(\Delta) := R^\alpha(\Delta) \cdot Area(\Delta)$$

Using the notations above, let

$$R_\alpha(t_{BD}) := R_\alpha(\Delta ABD) + R_\alpha(\Delta BCD).$$

Conjecture 1. *Suppose* $\alpha \geq 1$ *then* t_{BD} *is a Delaunay Triangulation* (DT) *if and only if* $R_\alpha(t_{BD}) \leq R_\alpha(t_{AC})$ *for all* $\alpha \geq 1$. t_{BD} *is DT, i.e.* $\angle A + \angle C < 180^\circ$ *if and only if* $R_\alpha(t_{BD}) < R_\alpha(t_{AC})$.

Theorem 8 (the case $\alpha = 1$)**.** *The conjecture is true for* $\alpha = 1$*, i.e.* t_{BD} *is DT if and only if* $S_A \cdot R_A + S_C \cdot R_C \leq S_B \cdot R_B + S_D \cdot R_D$

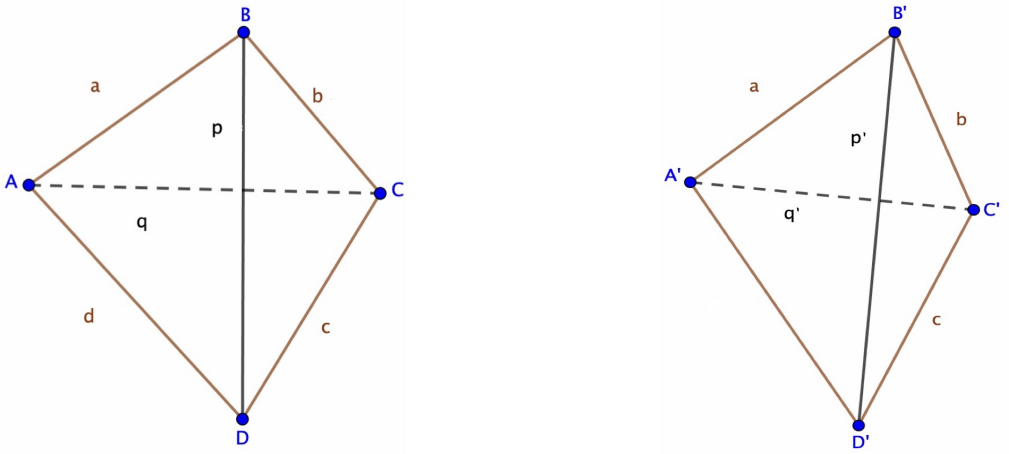

(a) $ABCD$ (b) $A'B'C'D'$

Figure 4.2: Quadrilaterals $ABCD$ and $A'B'C'D'$

Proof. Let sides a,b,c,d be fixed and increase p on Figure 4.2a. So $\tilde{p}(u)$ where $u \in [0,1]$ such that $\tilde{p}(0) = p$ and $\tilde{p}(1) = p'$. Then a quadrilateral A',B',C',D' with sides a,b,c,d and the diagonal $|B'D'| = p'$ is an inscribed quadrilateral , i.e. $\angle A' + \angle C' = \angle B' + \angle D' = 180^\circ$.

Note that for any triangle Δ with sides x,y,z, we have

$$R(\Delta) = \frac{x \cdot y \cdot z}{4 \cdot S_\Delta}.$$

Then $R(\Delta) \cdot S_\Delta = \frac{1}{4} x \cdot y \cdot z$. Now if we let $u \in [0,1]$, then we have the following notations:

$$S_A(u) = Area(a,d,\tilde{p}(u)) \qquad R_A(u) = R(a,d,\tilde{p}(u))$$

$$S_C(u) = Area(b,c,\tilde{p}(u)) \qquad R_C(u) = R(b,c,\tilde{p}(u))$$

$$S_B(u) = Area(a,b,\tilde{q}(u)) \qquad R_B(u) = R(a,b,\tilde{q}(u))$$

$$S_D(u) = Area(c,d,\tilde{q}(u)) \qquad R_D(u) = R(c,d,\tilde{q}(u))$$

$$f_p(u) = S_A(u)\cdot R_A(u) + S_C(u)\cdot R_C(u) \qquad f_q(u) = S_B(u)\cdot R_B(u) + S_D(u)\cdot R_D(u)$$

Therefore, $4(S_A \cdot R_A + S_C \cdot R_C) = p(ad+bc) = f_p(0)$. Other side follows, $4(S_B \cdot R_B + S_D \cdot R_D) = q(ab+cd) = f_q(0)$.

Now, let's consider $f_p(u)$ and $f_q(u)$. By definition, $\tilde{p}(u)$ is increasing then $\tilde{q}(u)$ is decreasing. Therefore, this implies that $f_p(u)$ is increasing and $f_q(u)$ is decreasing with u.

We know that $f_p(1) = f_q(1)$. Hence, for all $u \in [0,1]$, we have $f_p(u) \leq f_q(u)$. In particular, $f_p(0) \leq f_q(0)$ as required. □

4.2 R-vertices

R-vertices can be defined for any polygon. It is the circumradii where the circumradii is greater or equal to its neighbors or where the circumradii is less than or equal to its neighbors.

Suppose there is a polygon *ABCD* refer to Figure 4.1. Now, let there be a vertex B and neighbors A and C then R_B is the R-min if $R_A, R_C \geq R_B$. On the other hand, if $R_A, R_C \leq R_B$ then R_B is R-max. Moreover, we say that a convex quadrilateral *ABCD* is FRV (Four R–vertices) if $R_A \leq \min(R_B, R_D)$ and $R_C \leq \min(R_B, R_D)$. Now, We say that a convex quadrilateral *ABCD* is TRV (Two R–vertices) if $R_A \leq R_B \leq R_C \leq R_D$. We will need these definitions for the following lemmas and theorem.

Lemma 9 and 10 and Theorem 9 were first proved by O. R. Musin in 1997 [15].

Lemma 9. *Let $R_A \leq min(R_B, R_D)$. Then t_{BD} is DT, i.e. $\angle A + \angle C \leq 180^\circ$.*

Lemma 10. *If* $R_A \leq min(R_B, R_D)$ *then* $R_C \leq max(R_B, R_D)$.

Theorem 9. *Let* t_{BD} *is DT and* $R_A \leq R_C$ *or* $R_B \leq R_D$. *Then we have one of two cases:*

1. $R_A \leq R_C \leq R_B \leq R_D$ *or*

2. $R_A \leq R_B \leq R_C \leq R_D$

We can call a quadrilateral *ABCD* FRV (Four R-vertices) if we have *case I* and TRV (Two R-vertices) if we have a *case II*. Four R-vertices means there are two minimum and two maximum and Two R-vertices means there is one minimum and one maximum.

4.3 CRA–conjecture is true for FRV quadrilaterals

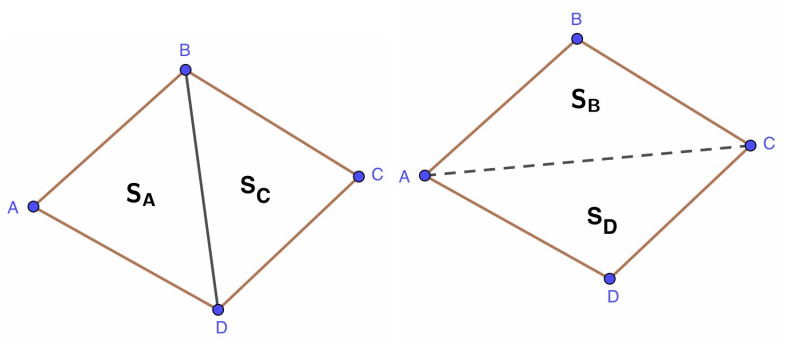

Figure 4.3: Area of *ABCD* triangulations

Theorem 10. *Suppose that a quadrilateral ABCD is FRV. Then the CRA conjecture is true for all* $\alpha > 0$.

Proof. It is easy to see (Fig. 4.3) that

$$S_A + S_C = S_B + S_D = \text{ Area}(ABCD).$$

Since $R_A \leq R_C \leq R_B \leq R_D$ we have

$$R_A^\alpha \cdot S_A + R_C^\alpha \cdot S_C \leq R_C^\alpha \cdot S_A + R_C^\alpha \cdot S_C = R_C^\alpha (S_A + S_C) = R_C^\alpha (S_B + S_D) \leq R_B^\alpha (S_B + S_D)$$

$$= R_B^\alpha \cdot S_B + R_B^\alpha \cdot S_D \le R_B^\alpha \cdot S_B + R_D^\alpha \cdot S_D$$

□

4.4 CRA–conjecture is true for TRV quadrilaterals with $S_A \ge S_B$

We have $S_A + S_C = S_B + S_D$. Then $S_A - S_B = S_D - S_C$.

Theorem 11. *Let $R_A \le R_B \le R_C \le R_D$.*

Suppose $S_A \ge S_B$. Then $R_A^\alpha \cdot S_A + R_C^\alpha \cdot S_C \le R_B^\alpha \cdot S_B + R_D^\alpha \cdot S_D$ for all $\alpha \ge 0$.

Proof. $S_A \cdot R_A^\alpha - S_B \cdot R_B^\alpha \le (S_A - S_B)R_B^\alpha \le (S_A - S_B)R_C^\alpha = (S_D - S_C)R_C^\alpha \le S_D \cdot R_D^\alpha - S_C \cdot R_C^\alpha$ as required. □

4.5 CRA–conjecture is true for TRV quadrilaterals with bounded R_C

Theorem 12. *If ABCD is TRV and*

$$R_C < \frac{R_B \cdot S_B + R_D \cdot S_D}{S_B + S_D}$$

then

$$R_A^\alpha \cdot S_A + R_C^\alpha \cdot S_C < R_B^\alpha \cdot S_B + R_D^\alpha \cdot S_D \ \text{ for all } \ \alpha \ge 1.$$

Proof. Jensen's inequality states that if f is a convex function, then for x_1, x_2 from its domain and $a_1 > 0$, $a_2 > 0$, we have

$$f\left(\frac{a_1 \cdot x_1 + a_2 \cdot x_2}{a_1 + a_2}\right) \le \frac{a_1 \cdot f(x_1) + a_2 \cdot f(x_2)}{a_1 + a_2}.$$

Note $f(x) = x^\alpha, \alpha \ge 1$ is convex. Thus,

$$\frac{R_B^\alpha \cdot S_B + R_D^\alpha \cdot S_D}{S_B + S_D} \ge \left(\frac{R_B \cdot S_B + R_D \cdot S_D}{S}\right)^\alpha > (R_C)^\alpha \ge \frac{R_C \cdot (S_C + S_A)}{S_C + S_A} \ge \frac{R_C^\alpha \cdot S_C + R_A^\alpha \cdot S_A}{S},$$

where $S = S_A + S_C = S_B + S_D$ □

4.6 Properties of TRV quadrilaterals

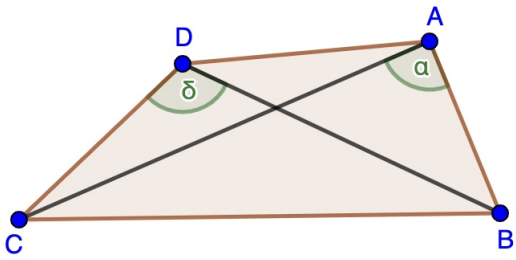

Figure 4.4: $ABCD$ where $\alpha = \angle BAC$ and $\delta = \angle BDC$.

Theorem 13 (Musin, 2009)**.** *$ABCD$ is TRV (i.e. $R_A < R_B < R_C < R_D$) if and only if* $180^\circ - \delta < \alpha < \delta$.

Hence, $\delta > 180^\circ - \delta \Rightarrow \delta > 90^\circ$ [14].

Proof. Let the angles of $ABCD$ satisfy the inequality above. Then $\sin\angle\alpha > \sin\angle\delta$ and therefore, $R_B < R_C$. Considering that $\angle\delta$ is obtuse, this implies that point A lies outside the circle BDC. Therefore, $\angle CAD < \angle CBD$. Since both of these angles are acute, then we have $\sin\angle CAD < \sin\angle CBD$ and $R_C < R_D$. Furthermore, we have that $\angle ACB < \angle ADB < 90^\circ$ therefore $R_A < R_B$.

On the contrary, from $R_B < R_C$ we get that $\angle\alpha$ lies between $\angle\delta$ and $180^\circ - \angle\delta$. If $\angle\delta$ is acute, then we have $\angle ABD < \angle ACD$. In addition, since $R_A < R_D$ then $\angle ABD > 180^\circ - \angle ACD$. However, in this scenario $R_B < R_A < R_D < R_C$ is obtained after repeating the previous argument. □

4.7 Examples to the CRA–Conjecture

Let us use the following function for our tables and graphs:

$$F(\alpha) = R_B^\alpha \cdot S_B + R_D^\alpha \cdot S_D - R_A^\alpha \cdot S_A - R_C^\alpha \cdot S_C$$

In this case, $ABCD$ is FRV and the inequality $F(\alpha)$ is greater than 0 for all $\alpha > 0$.

Example 1. Suppose there is a quadrilateral $ABCD$ where $a = b = c = d = 1$ and $p = 1$ (see figure 4.1).

Example 1 (FRV)				
Circumradius R_i and Area S_i	A	B	C	D
R	$\frac{\sqrt{3}}{3}$	$\sqrt{3}$	$\frac{\sqrt{3}}{3}$	$\sqrt{3}$
S	$\frac{\sqrt{3}}{4}$	$\frac{\sqrt{3}}{4}$	$\frac{\sqrt{3}}{4}$	$\frac{\sqrt{3}}{4}$

Table 4.1: Example 1 (FRV)

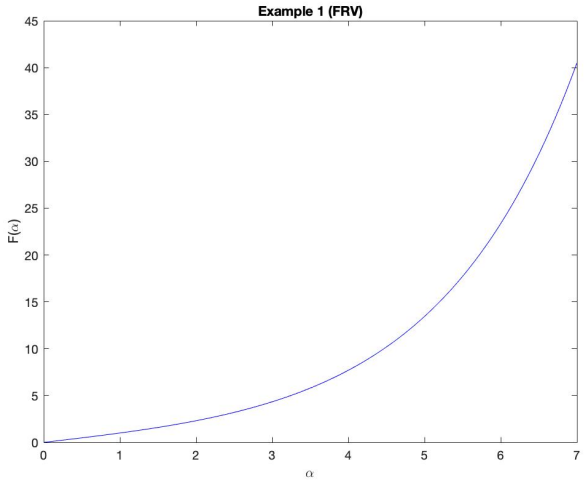

Figure 4.5: Four R-vertices example 1

Example 2 and 3 show that CRA conjecture is not true for $\alpha < 1$.

Example 2. Suppose there is a quadrilateral *ABCD* (see figure 4.4) where $a = d = c = 1, b = 2.91$ and $p = 1.9369$.

Example 2 (TRV)				
Circumradius R_i and Area S_i	A	B	C	D
R	2.0059	2.9243	5.1614	29.5458
S	0.2414	0.4975	0.273	0.0169

Table 4.2: Example 2 (TRV)

Example 3. Suppose there is a quadrilateral *ABCD* (see figure 4.4) where $a = d = c = 1, b = 2.99$ and $p = 1.9927$.

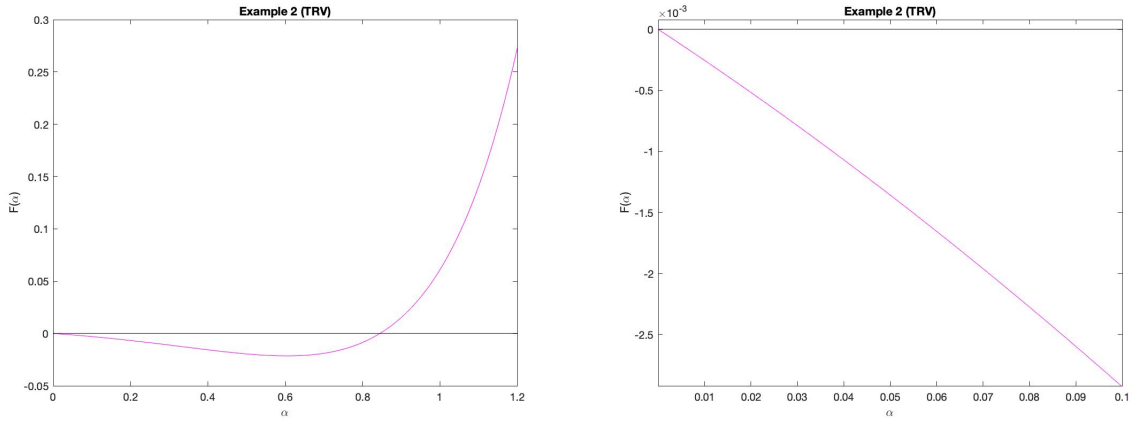

Figure 4.6: Left: Two R-vertices example 2. Right: Example 2 from [0,0.1].

Example 3 (TRV)				
Circumradius R_i and Area S_i	A	B	C	D
R	5.8769	8.6746	16.4749	175.8346
100S	8.477	17.2342	9.0415	0.2844

Table 4.3: Example 3 (TRV)

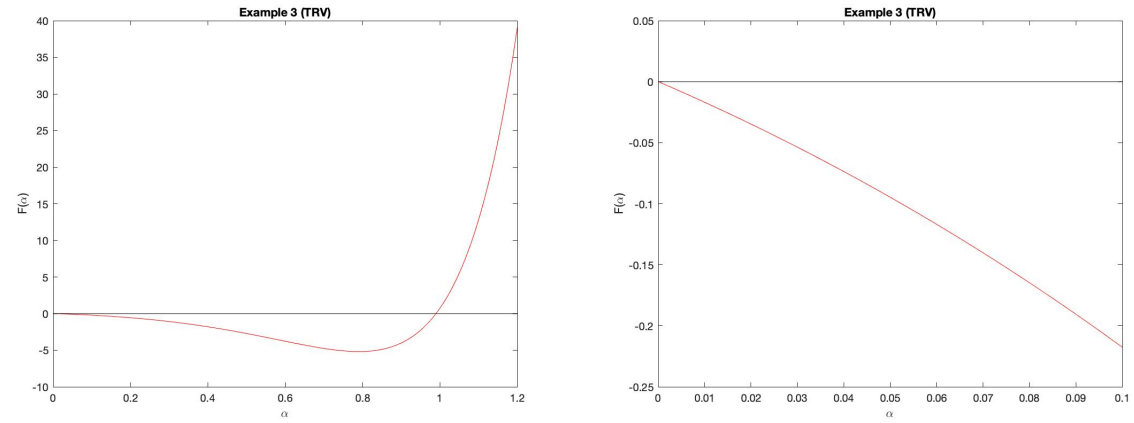

Figure 4.7: Left: Two R-vertices example 3. Right: Example 3 from [0,0.1].

CHAPTER V

CONCLUSION

In this paper, we studied the properties of Voronoi diagrams and its dual graph, Delaunay triangulations. These structures are highly discussed in computational geometry and have become great tools for many areas.

We started by discussing Voronoi diagrams and it's properties. We defined the Voronoi cell, edge, and vertex which are important definitions needed and referred to throughout the chapters to understand other properties. Following the definitions, several properties were explored such as a Voronoi diagram is a connected graph with edges that are line segments or half lines unless collinear, is made up of $2n-5$ vertices and $3n-6$ edges, and the characteristics of the largest empty circle. Moreover, we discuss two methods of construction. The first being the most basic one which is the Half Plane Intersection, and the second one being the Fortune's Algorithm. In the Fortune's Algorithm, we discussed two types of events that can occur during the construction of the Voronoi diagram.

Next, we developed the definitions and properties of the dual graph, Delaunay triangulations, by describing the duality between the two structures. We defined the dual as the straight line graph. Before defining the Delaunay triangulation, we begun by defining a triangulation and some properties such as the circumcircle property and empty circle test. These properties helped in arriving to the definition of a Delaunay triangulation. We then consider the case of four points and locally Delaunay. After that, we show the Flip Algorithm to demonstrate the construction of a Delaunay triangulation.

We continued with the discussion of Delaunay triangulations. Here, we examined the optimal functionals on triangulations and reductions to quadrilaterals. These include maximizing

the minimum angle criterion, lexicographical order of angle sequence, radii criterion, inradii criterion, harmonic index, weighted sum of squares of the edge lengths, Voronoi functional, and D functional. All these criterions and functionals are important because they prove to be useful in the study of algorithms and the development of optimal triangulations. They demonstrate whether Delaunay triangulation will be optimal or not. We then presented a new result. We proved the theorem that Delaunay triangulation has lexicographically the least circumradii sequence (see Theorem 3). We also discussed the CircumRadii-Area (CRA) conjecture.

We extended our research to this conjecture. We proved that the CRA conjecture was true for $\alpha = 1$. We did this by fixing the sides of a quadrilateral *ABCD* and increasing the segment *BD*. We ended up getting a new quadrilateral $A'B'C'D'$. The circumradius formula was required to complete the proof. We were able to demonstrate that the conjecture was true for $\alpha = 1$.

We carried on with this conjecture and proved that CRA conjecture was true for FRV quadrilaterals. FRV quadrilaterals are where $R_A \leq R_C \leq R_B \leq R_D$. We showed that $R_\alpha(t_{BD}) \leq R_\alpha(t_{AC})$ was true for all $\alpha > 0$. This was proved by showing that $R_A^\alpha \cdot S_A + R_C^\alpha \cdot S_C \leq R_B^\alpha \cdot S_B + R_D^\alpha \cdot S_D$.

The following step that was taken was proving that CRA conjecture was true for TRV quadrilaterals with $S_A \geq S_B$. TRV quadrilaterals are where $R_A \leq R_B \leq R_C \leq R_D$. We were able to show this by $S_A \cdot R_A^\alpha - S_B \cdot R_B^\alpha \leq S_D \cdot R_D^\alpha - S_C \cdot R_C^\alpha$.

We proved that CRA conjecture was true for TRV quadrilaterals with bounded R_C. This proof was completed using the Jensen's inequality.

We show the properties of TRV quadrilaterals. We use Theorem 13 proved by Musin to demonstrate that a quadrilateral is TRV iff $180^\circ - \angle BDC < \angle BAC < \angle BDC$. This implies that $\angle BDC$ is greater than 90°.

Lastly, we demonstrated counterexamples for $\alpha < 1$. These are table 4.2 and table 4.3, and along with them, we provided graphs. We added a secondary graph for both of these examples to show that it is not tangent to zero.

5.1 Status of CRA–conjecture

Now, let's combine all the properties of *ABCD* together that remain to prove the conjecture.

I. $R_A \leq R_B \leq R_C \leq R_D$.

II. $S_A - S_B = S_D - S_C < 0$.

III. $R_C \cdot S > R_B \cdot S_B + R_D \cdot S_D$, where $S = \text{Area}(ABCD) = S_A + S_C = S_B + S_D$.

IV. (See Theorem 8)

$R_A \cdot S_A + R_C \cdot S_C \leq R_B \cdot S_B + R_D \cdot S_D$.

V. (See [7])

$R_A^2 \cdot S_A + R_C^2 \cdot S_C \leq R_B^2 \cdot S_B + R_D^2 \cdot S_D$.

Proposition 2. *Let ABCD is TRV and $R_C \cdot S_C > R_D \cdot S_D$. Then we have II.*

Proof. Let's assume the contrary, $S_C < S_D$. In this case, by I, we have that $R_C < R_D$ which implies that $R_C \cdot S_C < R_D \cdot S_D$. By contradiction, if *ABCD* is TRV and $R_C \cdot S_C > R_D \cdot S_D$ then $S_D < S_C$. □

It remains to prove our theorem for quadrilaterals with these properties. This is due to these properties being complements for the proved theorems. For instance, the CRA conjecture is proved for FRV, but it remains to prove the conjecture for non-FRV quadrilaterals, that is TRV quadrilaterals. The CRA conjecture is proved for $S_A > S_B$, it remains to prove for $S_A < S_B$. The conjecture is proved for $R_C < \frac{R_B \cdot S_B + R_D \cdot S_D}{S_B + S_D}$, it remains to prove for $R_C > \frac{R_B \cdot S_B + R_D \cdot S_D}{S_B + S_D}$.

5.2 Discussion

In this thesis, we were able to proved various theorems showing that the CRA conjecture held true as previously mentioned. We can conclude that R_α where $\alpha = 1$ attains its minimum at the Delaunay triangulation. We can also conclude that for FRV quadrilaterals R_α where $\alpha > 0$ attains its minimum at the Delaunay triangulation. Similarly, for TRV quadrilaterals with $S_A \geq S_B$, R_α where $\alpha \geq 0$ attains its minimum at the Delaunay triangulation. Additionally, for TRV quadrilaterals with bounded R_C, R_α where $\alpha \geq 1$ attains its minimum at the Delaunay triangulation. These cases are important because they demonstrate that the Delaunay triangulation is optimal when $\alpha \geq 1$ in the CRA conjecture.

However, it is not complete. There is still some work that needs continuation, and it would be interesting to see where that leads us. As all these functionals and criteria help us to construct optimal triangulations which are useful in a variety of fields.

BIBLIOGRAPHY

[1] O. ARSLAN, *Clustering-Based Robot Navigation and Control*, PhD thesis, 2016.

[2] F. AURENHAMMER AND R. KLEIN, *Voronoi diagrams.*, Handbook of computational geometry, Vol. 5 (2000), pp. 201–290.

[3] D. AUSTIN, *Voronoi diagrams and a day at the beach*, URL: http://www. ams. org/samplings/feature-column/fcarc-voronoi, (2006).

[4] S.-W. CHENG, T. K. DEY, AND J. SHEWCHUK, *Delaunay mesh generation*, CRC Press, 2012.

[5] B. DELAUNAY ET AL., *Sur la sphere vide*, Izv. Akad. Nauk SSSR, Otdelenie Matematicheskii i Estestvennyka Nauk, Vol. 7 (1934), pp. 793–800.

[6] S. DRYSDALE, *Voronoi diagrams: Applications from archaology to zoology*, Regional Geometry Institute, Smith College, (1993).

[7] H. EDELSBRUNNER, A. GLAZYRIN, O. R. MUSIN, AND A. NIKITENKO, *The voronoi functional is maximized by the delaunay triangulation in the plane*, Combinatorica, Vol. 37 (2017), pp. 887–910.

[8] B. GÄRTNER AND M. HOFFMANN, *Computational geometry lecture notes hs 2013*, ETH Zürick, (2013).

[9] T. LAMBERT, *The delaunay triangulation maximizes the mean inradius.*, in Proc. 6thCanad. Conf. Comput. Geom., Citeseer, 1994, pp. 201–206.

[10] C. L. LAWSON, *Software for c1 surface interpolation*, in Mathematical software, Elsevier, 1977, pp. 161–194.

[11] T. M. LIEBLING AND L. POURNIN, *Voronoi diagrams and delaunay triangulations: Ubiquitous siamese twins*, 2012.

[12] D. M. MOUNT, *Cmsc 754 computational geometry*, (2002).

[13] M. MUMM, *Voronoi diagrams*, The Mathematics Enthusiast, Vol. 1 (2004), pp. 44–55.

[14] O. MUSIN, *Sharygin geometry olympiad v.2*, (2007-2019), pp. 210–211.

[15] O. R. MUSIN, *Properties of the delaunay triangulation*, in Proceedings of the thirteenth annual symposium on Computational geometry, 1997, pp. 424–426.

[16] S. C. NANDY, *Voronoi diagram*, Advanced Computing and Microelectronics Unit Indian Statistical Institute Kolkata, (2007).

[17] V. T. RAJAN, *Optimality of the delaunay triangulation in* $\mathbb{R}^d$, Discrete & Computational Geometry, Vol. 12 (1994), pp. 189–202.

[18] R. SIBSON, *Locally equiangular triangulations*, The computer journal, Vol. 21 (1978), pp. 243–245.

[19] M. VAN KREVELD, O. SCHWARZKOPF, M. DE BERG, AND M. OVERMARS, *Computational geometry algorithms and applications*, Springer, 2000.

BIOGRAPHICAL SKETCH

Estefania Sierra was born on December 31, 1996 in Brownsville, Texas. She attended Morningside Elementary and Lucio Middle School where she was a consistent honor student with perfect attendance that played sports. She was invited to join the National Junior Honor Society due to her scholastic work. She then attended Lopez High School. There she became involved in a lot of clubs. She was the vice president for Zonta Z Club, and a member for the book club, VITA club, Spanish Honor Society, and National Honor Society. Her honors followed her into high school where she was top 5% of her class. She started taking Dual Enrollment and AP classes to get college credit. After completing her schoolwork at Lopez High School, she graduated with honors on June 2015. On August 2015, Estefania started her first semester at The University of Texas Rio Grande Valley in Brownsville, Texas. She was consistently awarded with the President's List throughout her college career. She joined the STEMS Mentor Club her sophomore year and soon after became the secretary of the club. She was also the secretary of the Gorgas Science Society. Estefania worked for Closing the G.A.P.S and Science of Mechanical Applications and Related Technology Summer Camp at TSC. She also worked for Texas Pre-Freshman Engineering Program and High Scholars Summer Program at UTRGV. In the spring of 2019, she began an accelerated degree program called (4+1) BS/MS. The program would allow her to get an early start on her Master's degree while completing her Bachelor's degree. She was then offered a job as a graduate assistant and worked as one for about two years. Estefania received a Bachelor of Science in Mathematics on December 2020 from the University of Texas Rio Grande Valley. On May 2021, Estefania was awarded a Master of Science in Mathematics from the University of Texas Rio Grande Valley.

For more information contact Estefania Sierra at estefania.aide.sierra01@gmail.com